Electronic Supplementary Material (ESI) for Polymer Chemistry.
This journal is © The Royal Society of Chemistry 2022

Supporting Information for

Facile Synthesis of Epoxide-co-Propylene Sulphide Polymers with Compositional and Architectural Control

Niloofar Safaie[1], Jessica Smak[2], Danielle DeJonge[2], Shiwang Cheng[2], Xiaobing Zuo[3], Kohji Ohno*[4], Robert C. Ferrier, Jr.*[2]

1. Department of Chemistry, Michigan State University, East Lansing, Michigan 48824, United States, 2. Department of Chemical Engineering and Materials Science, Michigan State University, East Lansing, Michigan 48824, United States, 3. X-ray Science Division, Argonne National Laboratory, Lemont, Illinois, 604393, 4. Institute for Chemical Research, Kyoto University, Kyoto 611-0011, Japan.

Table of contents

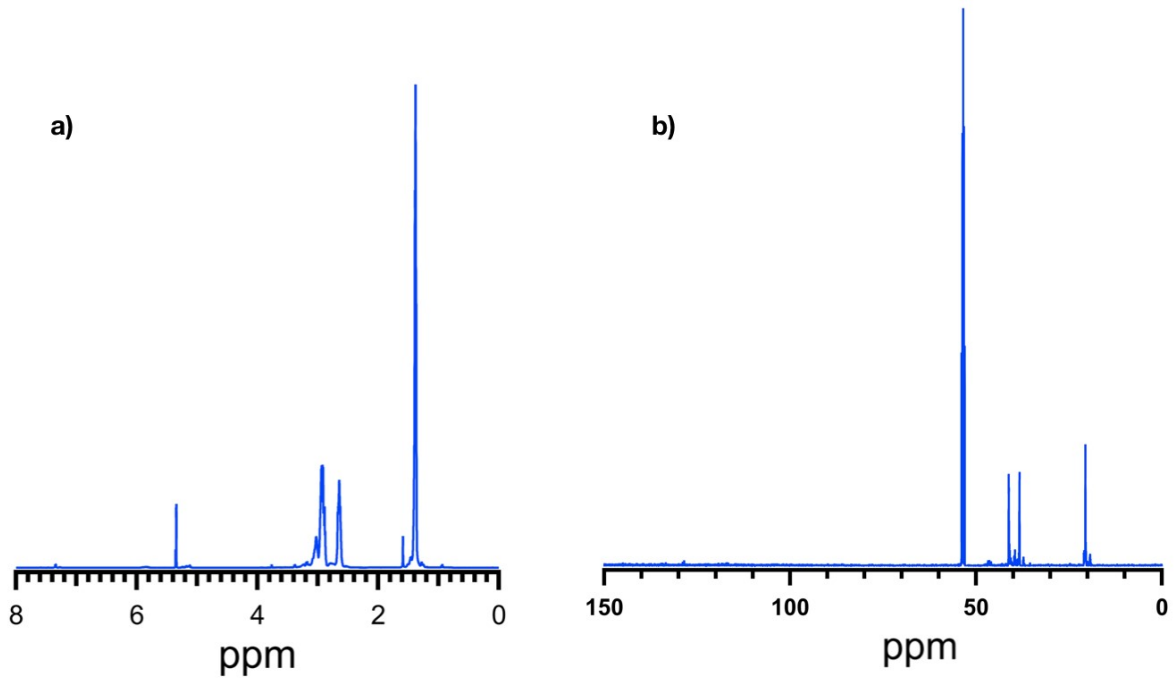

Figure S 1 ^{1}H NMR and ^{13}C NMR spectra of BnSPPS. a) ^{1}H NMR (500 MHz, $CDCl_3$) δ 2.91-2.80 (m, −S−C<u>H</u>$_2$−CH(CH_3)−S−), 2.65-2.58 (m, −S−CH_2−C<u>H</u>(CH_3)−S−), 1.39 (m, −S−CH_2−CH(C<u>H</u>$_3$)−S−). b) ^{13}C NMR (126 MHz, $CDCl_3$) δ 41.14 (−S−CH_2−<u>C</u>H(CH_3)−S), 38.18 (−S−<u>C</u>H$_2$−CH(CH_3)−S), 20.63 (−S−CH_2−CH(<u>C</u>H$_3$)−S−).

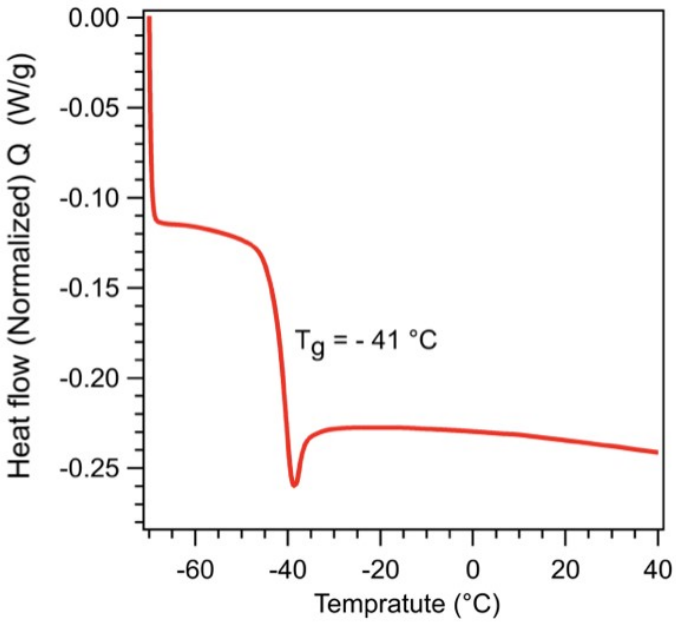

Figure S 2 DSC analysis of targeted 30k PPS with $BnSAlMe_2$. The data from the second heating curve were collected which reveals one Tg at -41 °C.

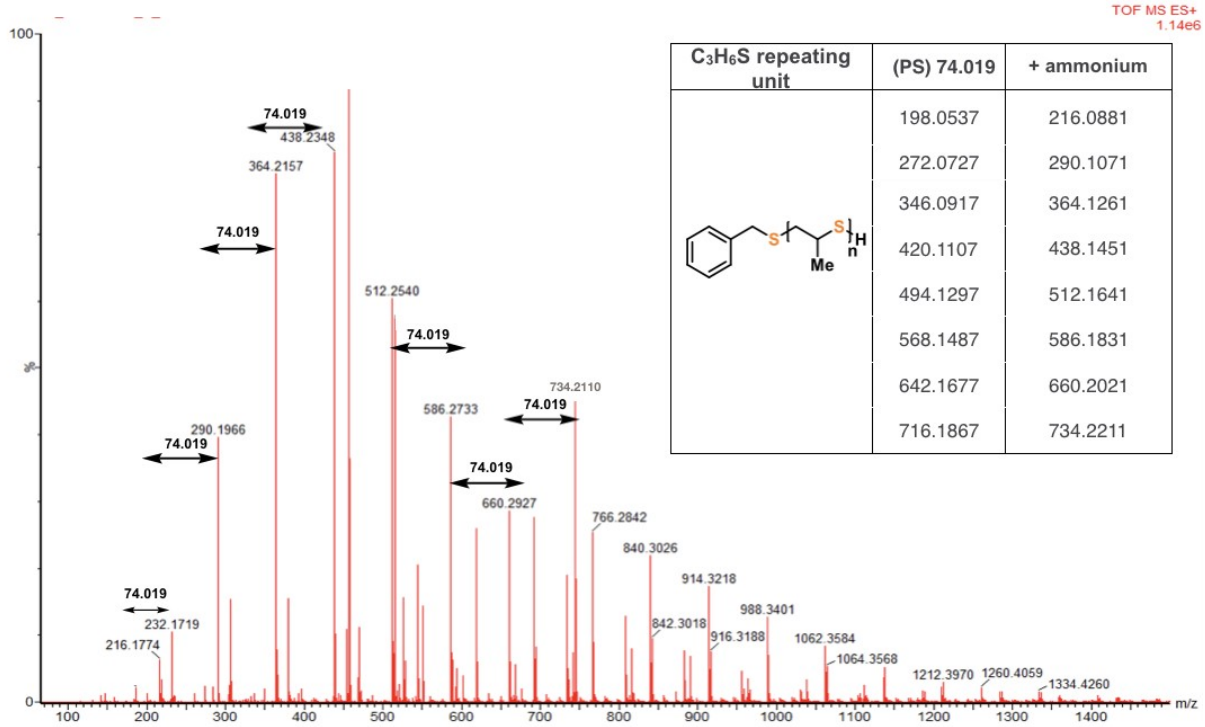

C_3H_6S repeating unit	(PS) 74.019	+ ammonium
	198.0537	216.0881
	272.0727	290.1071
	346.0917	364.1261
	420.1107	438.1451
	494.1297	512.1641
	568.1487	586.1831
	642.1677	660.2021
	716.1867	734.2211

Figure S 3 ESI-MS characterization of the targeted 5kg/mol PPS.

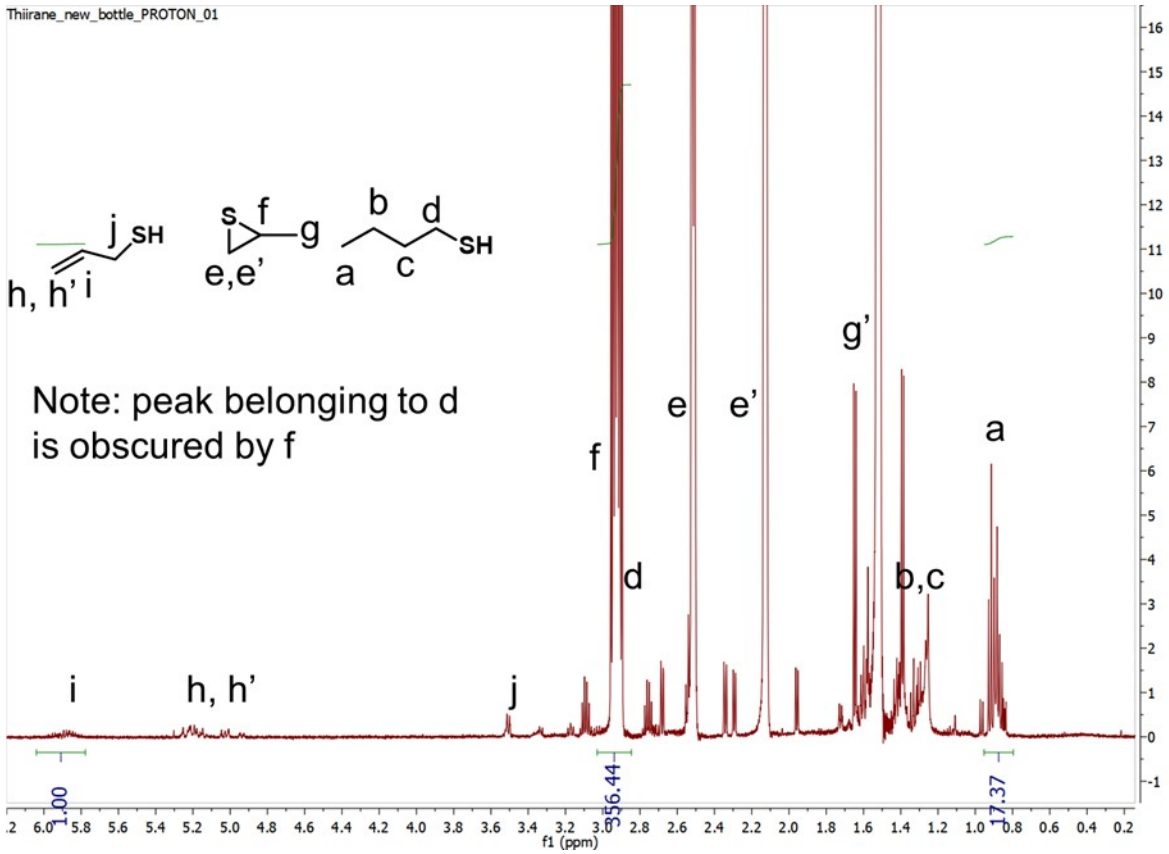

Figure S 4 ^{1}H NMR spectrum of propylene sulfide monomer. Three species are present consisting of propylene sulfide (majority), butane thiol (ca. 1.6 mol%), propene thiol (ca. 0.28 mol%).

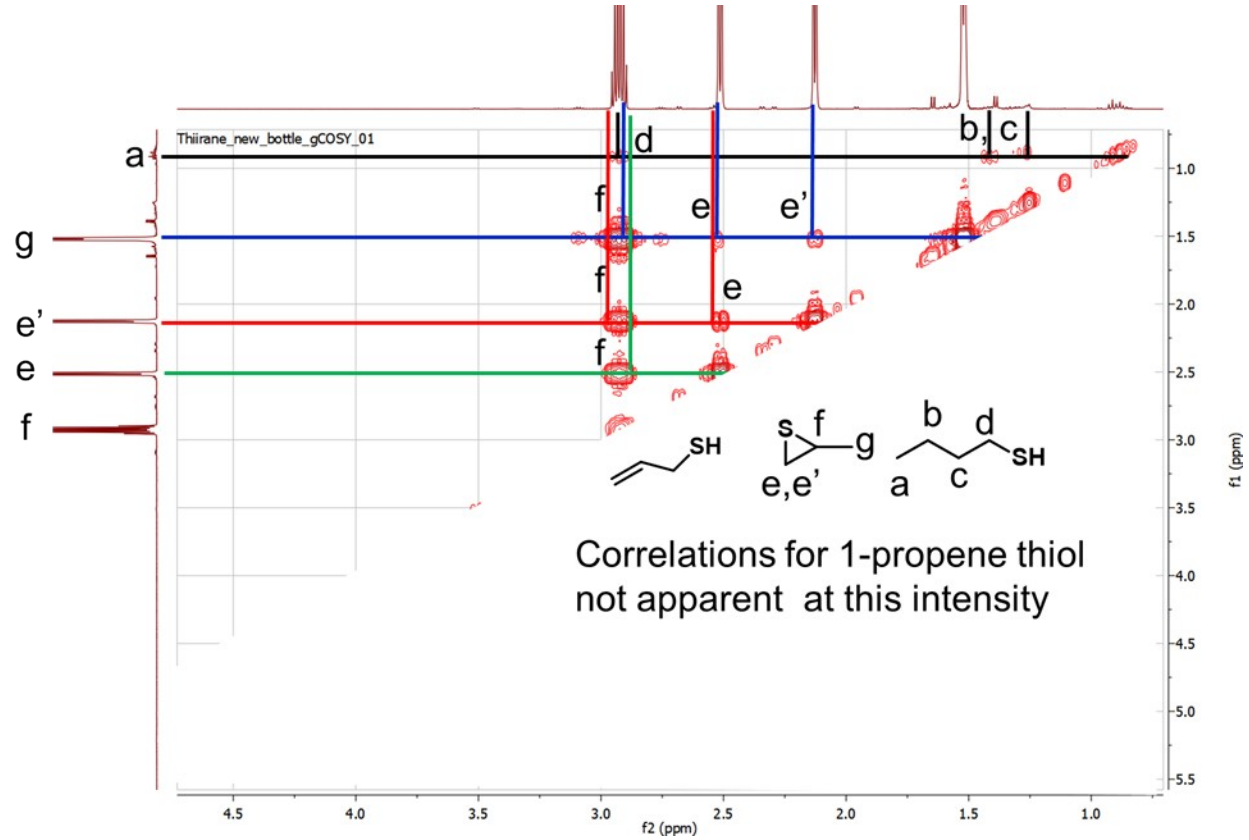

Figure S 5. COSY spectrum of PS monomer. At this intensity, clear correlations consistent with propylene sulfide and butane thiol are present.

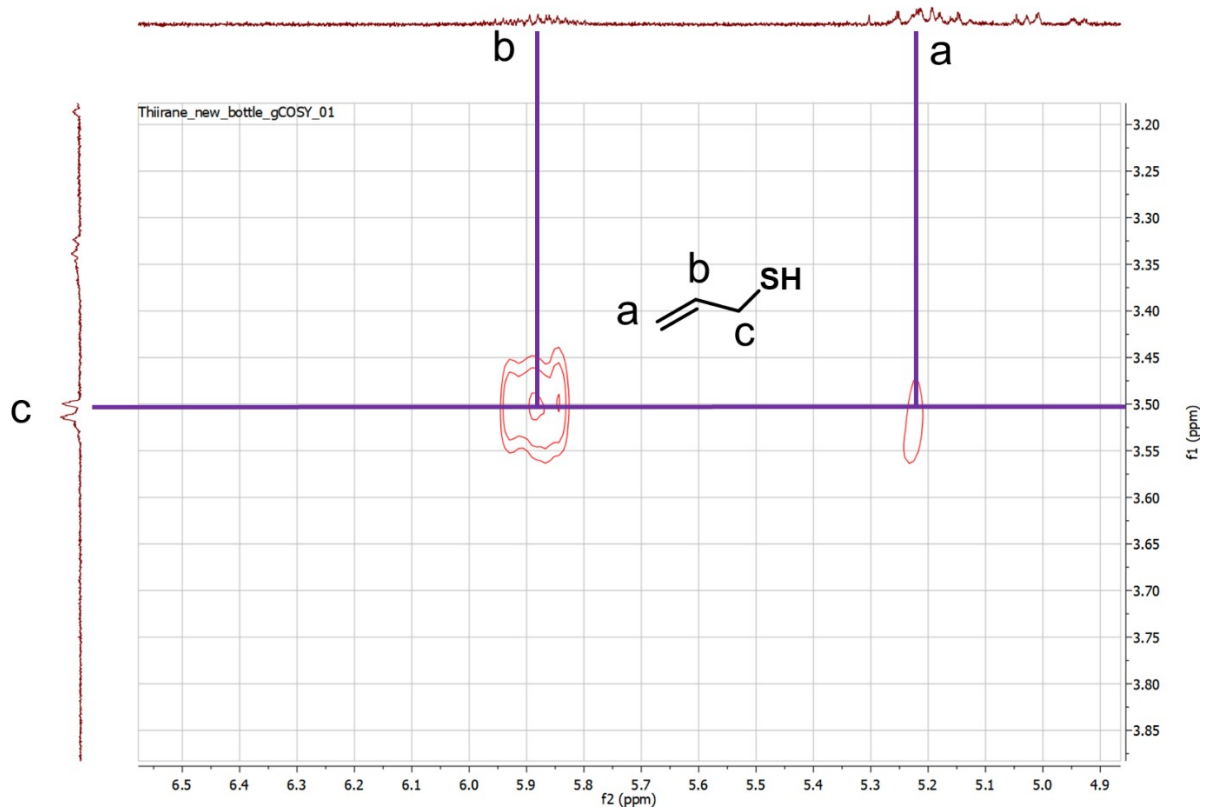

Figure S 6. COSY spectrum of PS monomer showing correlation peaks between protons adjacent to a sulfur and protons associated with allyl group, consistent with propene thiol.

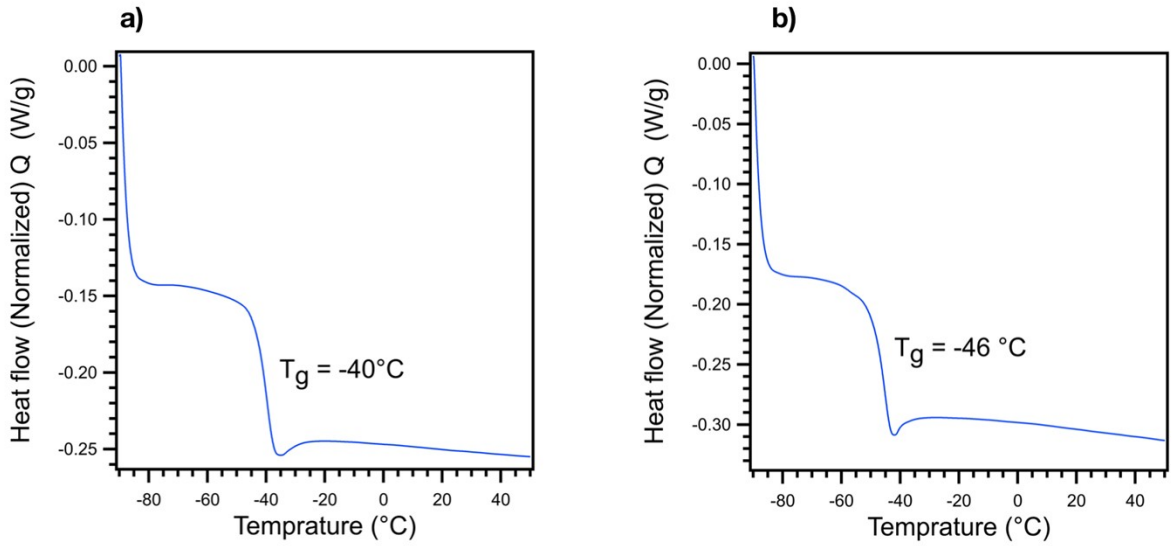

Figure S 7 DSC analysis of (a) poly(ECH-*stat*-PS) and (b) poly(PO-*stat*-PS). The data from the second heating curve were collected which reveals one Tg at -40 °C for poly(ECH-*stat*-PS) and one Tg at -46 °C for poly(PO-*stat*-PS).

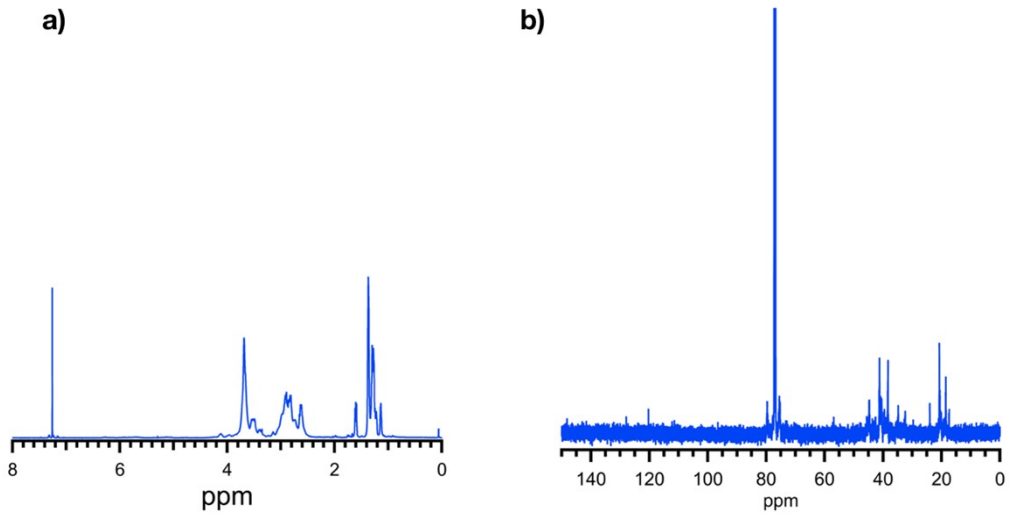

Figure S 8 ^{1}H NMR and ^{13}C NMR spectra of poly(ECH-*stat*-PS). a) ^{1}H NMR (500 MHz, $CDCl_3$) δ 3.80-3.29 (bm, −O−C<u>H</u>$_2$−C<u>H</u>(C<u>H</u>$_2$Cl)−O−), 3.16-2.51 (bm, −S−C<u>H</u>$_2$−C<u>H</u>(CH_3)−S−), 1.63-1.54 (m, −O−CH_2−C<u>H</u>(CH_2Cl)−O− and −S−CH_2−C<u>H</u>(CH_3)−S−), 1.40-1.33 (m, −S−CH_2−CH(C<u>H</u>$_3$)−S−), 1.37-1.17 O−C<u>H</u>$_2$−CH(CH_2Cl)−O− and −S−C<u>H</u>$_2$−CH(CH_3)−S−). b) ^{13}C NMR (126 MHz, $CDCl_3$) 79.37(−O−CH_2−<u>C</u>H(CH_2Cl)−O−), 75.58 (−O−<u>C</u>H_2−CH(CH_2Cl)−O−), 44.72 (−O−CH_2−CH(<u>C</u>H_2Cl)−O−), 41.16 (−S−CH_2−<u>C</u>H(CH_3)−S−), 38.39 (−O−CH_2−<u>C</u>H(CH_2Cl)−O− and −S−CH_2−<u>C</u>H(CH_3)−S−), 20.63 (−S−<u>C</u>H_2−CH(CH_3)−S−), 20.85 (−O−<u>C</u>H_2−CH(CH_2Cl)−O− and −S−<u>C</u>H_2−CH(CH_3)−S−), 18.59 (−S−CH_2−CH(<u>C</u>H_3)−S−).

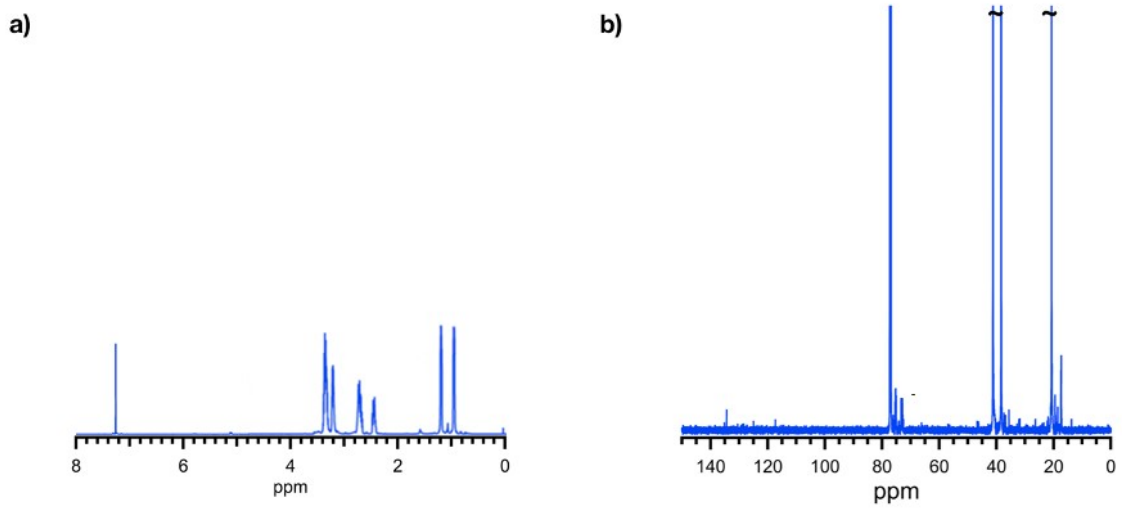

Figure S 9 ^{1}H NMR and ^{13}C NMR spectrum of poly(PO-*stat*-PS). (a) ^{1}H NMR (500 MHz, $CDCl_3$) δ 3.83-3.24 (bm, −O−C<u>H</u>$_2$−C<u>H</u>(CH_3)−O−), 3.10-2.41 (bm, −S−C<u>H</u>$_2$−C<u>H</u>(CH_3)−S−, −O−CH_2−C<u>H</u>(CH_3)−O− and −S−CH_2−C<u>H</u>(CH_3)−S−), 1.32-1.42 (m, −S−CH_2−CH(C<u>H</u>$_3$)−S−), 1.30-1.19 (bm, −O−C<u>H</u>$_2$−CH(CH_3)−O− and −S−C<u>H</u>$_2$−CH(CH_3)−S−), 1.17-1.04 (m, −O−CH_2−CH(C<u>H</u>$_3$)−O−). (b) ^{13}C NMR (126 MHz, $CDCl_3$) δ75.85 (−O−CH_2−<u>C</u>H(CH_3)−O−), 73.34 (−O−<u>C</u>H_2−CH(CH_3)−O−), 72.90 (−O−CH_2−<u>C</u>H(CH_3)−O− and −S−CH_2−<u>C</u>H(CH_3)−S), 41.23 (−S−CH_2−<u>C</u>H(CH_3)−S−), 38.10 (−S−<u>C</u>H_2−CH(CH_3)−S−), 20.8 (−O−<u>C</u>H_2−CH(CH_3)−O− and −S−<u>C</u>H_2−CH(CH_3)−S), 19.3 (−S−CH_2−CH(<u>C</u>H_3)−S−), 17.4 (−O−CH_2−CH(<u>C</u>H_3)−O−).

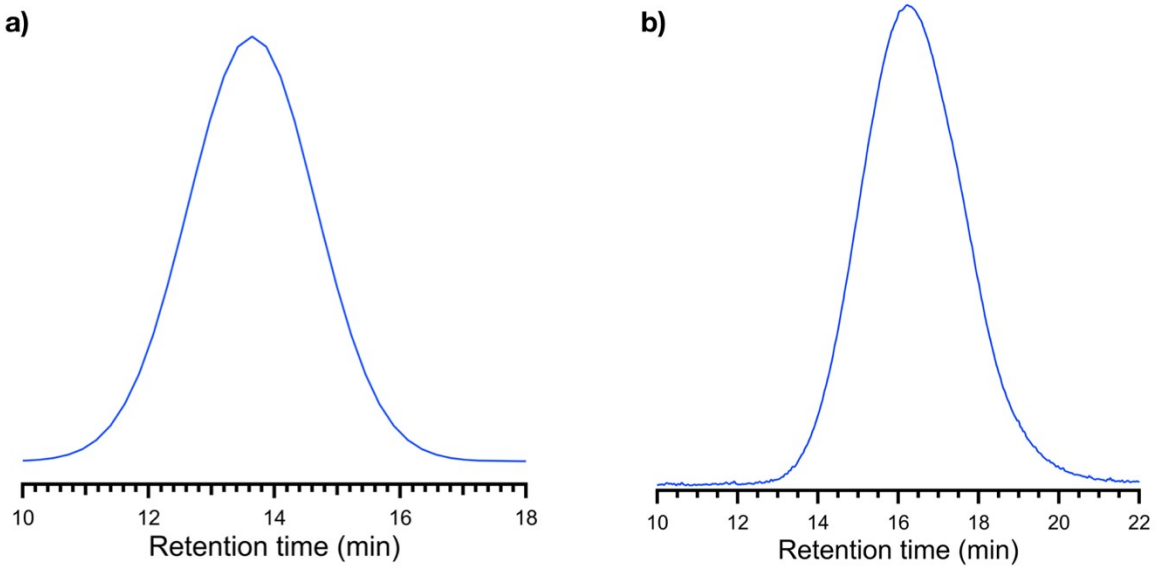

Figure S 10 SEC traces of (a) poly(ECH-*stat*-PS) and (b) poly(PO-*stat*-PS). For poly(ECH-stat-PS), the M_n is determined to be 29.2 kg/mol with Đ of 1.56. And for or poly(PO-stat-PS), the M_n is determined to be 30.8 kg/mol with Đ of 1.21.

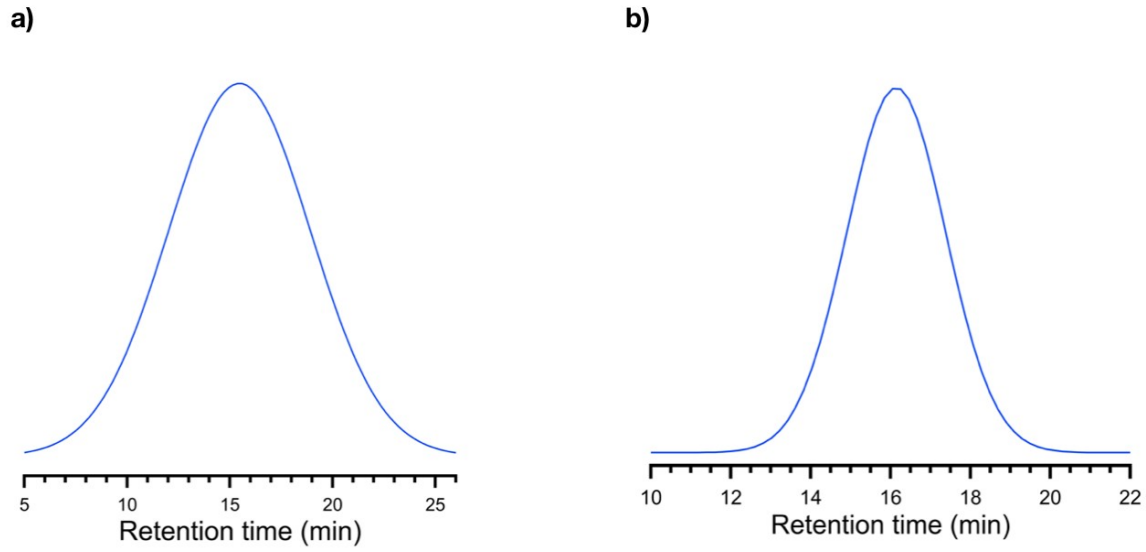

Figure S 11 SEC traces of (a) P(ECH-*b*-PS) and (b) P(PO-*b*-PS). For poly(ECH-*b*-PS), the M_n is determined to be 29.9 kg/mol with Đ of 1.74. And for poly(PO-*b*-PS), the M_n is determined to be 29.6 kg/mol with Đ of 1.32. And

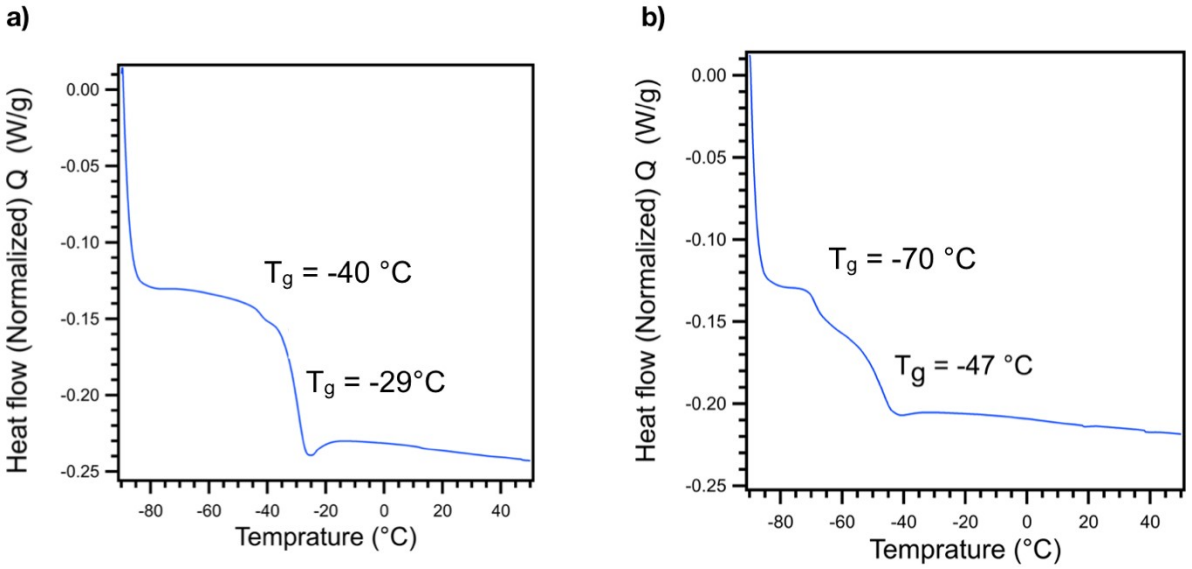

Figure S 12 DSC analysis of (a) poly(ECH-*b*-PS) and (b) poly(PO-*b*-PS). The data from the second heating curve were collected which reveals two Tg at -40 °C and -29 °C for PPS and PECH blocks, respectively. For poly(PO-b-PS) two Tg at -70 °C and -47 °C for PPO and PPS blocks, respectively.

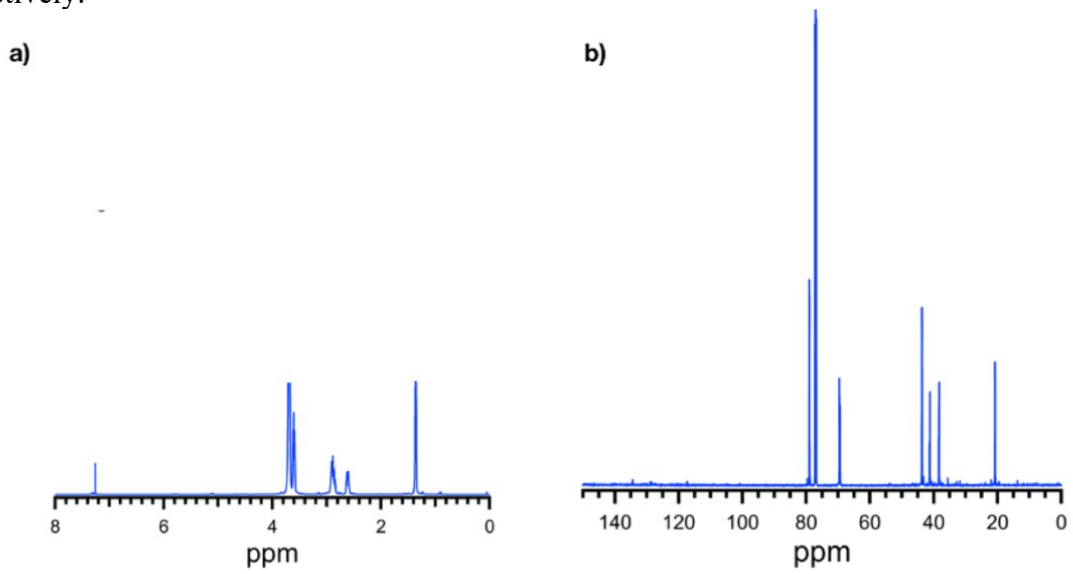

Figure S 13 ^{1}H NMR and ^{13}C NMR spectrum of poly(ECH-*b*-PS). (a) ^{1}H NMR (500 MHz, $CDCl_3$) δ 3.77-3.55 (bm, −O−C$\underline{H}_2$−C$\underline{H}$(C$\underline{H}_2$Cl)−O−), 2.91-2.80 (m, −S−C$\underline{H}_2$−CH(CH_3)−S−), 2.65-2.58 (m, −S−CH_2−C$\underline{H}$(CH_3)−S−), 1.35 (m, −S−CH_2−CH(C$\underline{H}_3$)−S−). (b) ^{13}C NMR (126 MHz, $CDCl_3$) δ 78.97 (−O−CH_2−$\underline{C}$H(CH_2Cl)−O−), 69.51 (−O−$\underline{C}H_2$−CH(CH_2Cl)−O), 43.47 (−O−CH_2−CH(C$\underline{H}_2$Cl)−O−), 41.17 (−S−CH_2−$\underline{C}$H(CH_3)−S−), 38.24 (−S−$\underline{C}H_2$−CH(CH_3)−S−), 20.86 (−S−CH_2−CH(C$\underline{H}_3$)−S−).

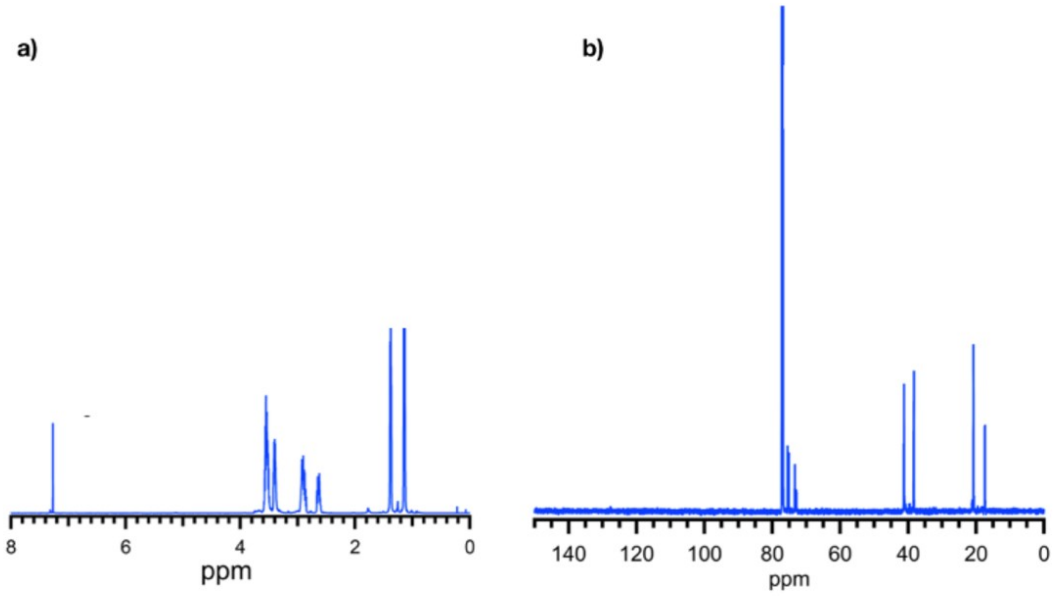

Figure S 14 ^{1}H NMR and ^{13}C NMR spectrum of poly(PO-*b*-PS). (a) ^{1}H NMR (500 MHz, $CDCl_3$) δ 3.72−3.2 (bm, −O−C$\underline{H}_2$−C$\underline{H}$(CH_3)−O−), 2.91-2.54 (bm, −S−C$\underline{H}_2$−C$\underline{H}$(CH_3)−S−), 1.31 (m, −S−CH_2−CH(C$\underline{H}_3$)−S−), 1.11 (m, −O−CH_2−CH(C$\underline{H}_3$)−O−). (b) ^{13}C NMR (126 MHz, $CDCl_3$) δ 75.26 (−O−CH_2−$\underline{C}$H(CH_3)−O−), 73.35 (−O−$\underline{C}H_2$−CH(CH_3)−O−), 40.6 (−S−CH_2−$\underline{C}$H(CH_3)−S−), 37.9 (−S−$\underline{C}H_2$−CH(CH_3)−S−), 20.98 (−S−CH_2−CH($\underline{C}H_3$)−S−), 16.83 (−O−CH_2−CH($\underline{C}H_3$)−O−).

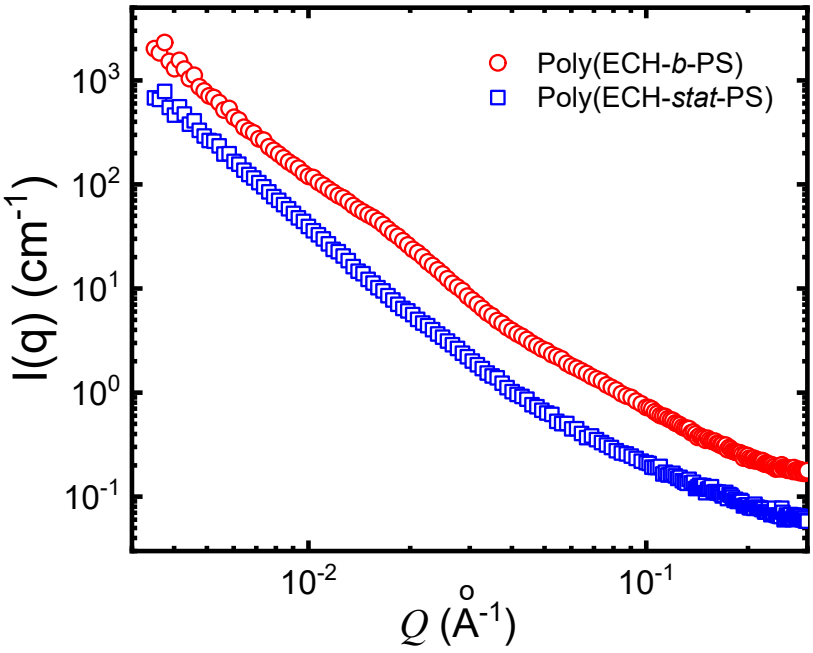

Figure S 15 SAXS data for P(ECH-b-PS) and P(ECH-stat-PS). Small-angle x-ray scattering (SAXS) revealed a weak shoulder peak at Q ~0.015 Å^{-1}, indicating weak phase separation behavior for P (ECH-b-PS) block copolymer.

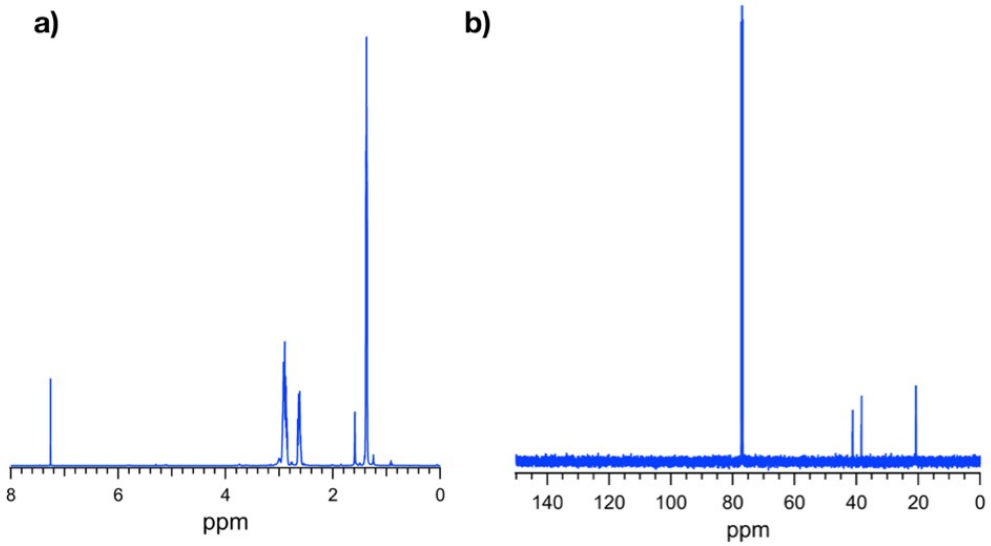

Figure S 16 ^{1}H NMR and ^{13}C NMR spectra of BnOPPS. a) ^{1}H NMR (500 MHz, $CDCl_3$) δ 2.91-2.80 (m, −S−C<u>H</u>$_2$−CH(CH_3)−S−), 2.65-2.58 (m, −S−CH_2−C<u>H</u>(CH_3)−S−), 1.39 (m, −S−CH_2−CH(C<u>H</u>$_3$)−S−). b) ^{13}C NMR (126 MHz, $CDCl_3$) δ 41.14 (−S−CH_2−<u>C</u>H(CH_3)−S), 38.18 (−S−<u>C</u>H_2−CH(CH_3)−S), 20.63 (−S−CH_2−CH(<u>C</u>H_3)−S−).

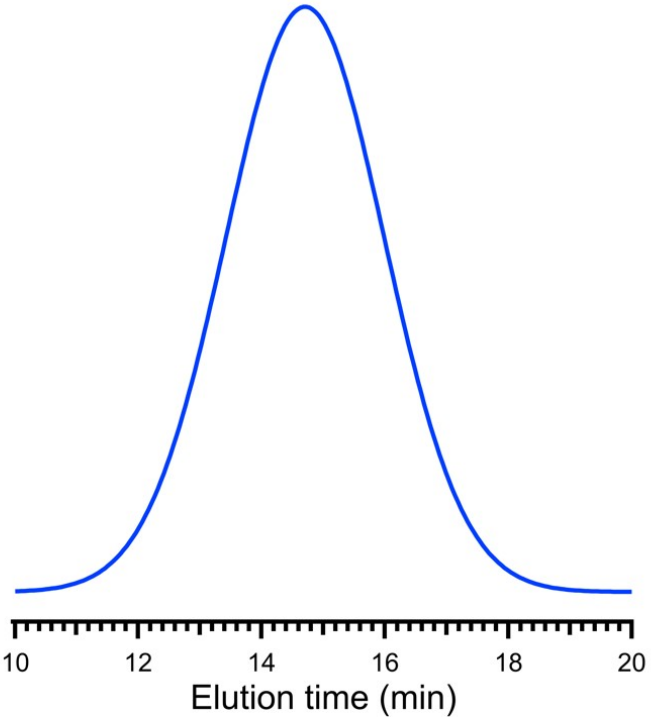

Figure S 17 SEC trace of targeted 30k BnOPPS. the M_n is determined to be 31.6 kg/mol with Đ of 1.32.

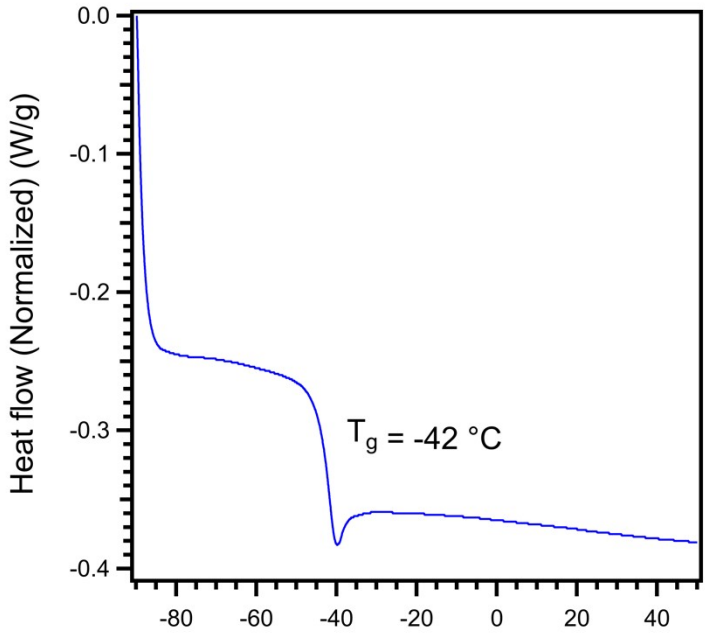

Figure S 18 DSC trace of BnOPPS. The data from the second heating curve were collected which reveals one Tg at -42 °C.

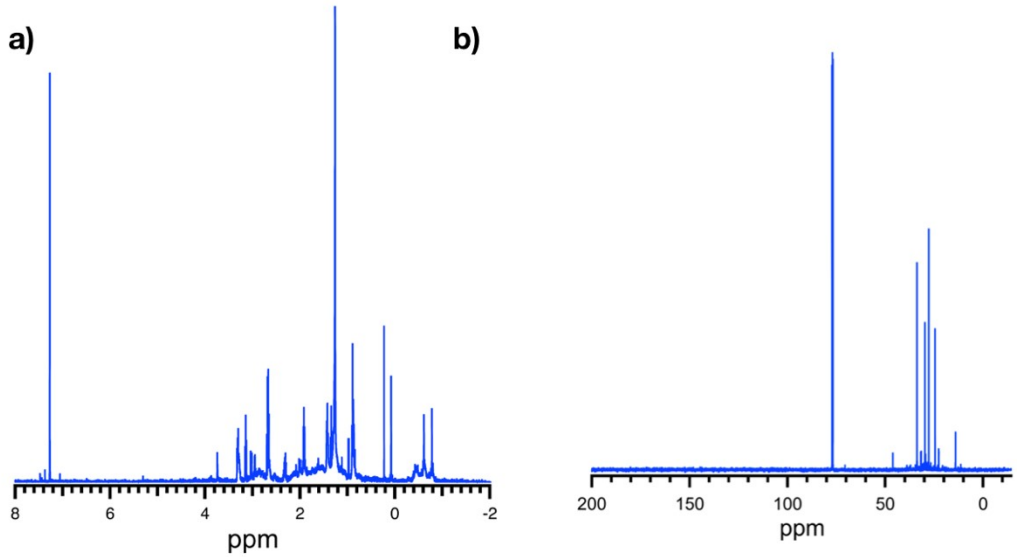

Figure S 19^{1}H NMR and ^{13}C NMR spectra of d-H initiator. (a) ^{1}H NMR (500 MHz, $CDCl_3$) δ 1.7-3.41 (b, $_2(CH_3)$Al-C$\underline{H_2}$C$\underline{H_2}$C$\underline{H_2}$S-Al$(CH_3)_2$, 6H), -0.92-0.24 (b, $_2(C\underline{H_3})$Al-$CH_2CH_2CH_2$S-Al$(C\underline{H_3})_2$, 6H). Peaks at 0.88 and 1.26 in ^{1}H NMR spectrum, are corresponded to hexane. (b) ^{13}C NMR (126 MHz, $CDCl_3$) δ 29.65 $_2(CH_3)$Al-$\underline{C}H_2CH_2\underline{C}H_2$S-Al$(CH_3)_2$, 27.73 $_2(CH_3)$Al-$CH_2\underline{C}H_2CH_2$S-Al$(CH_3)_2$, 11.31$_2(\underline{C}H_3)$Al-$CH_2CH_2CH_2$S-Al$(\underline{C}H_3)_2$. Peaks at 14.14, 22.53, and 33.8 in ^{13}C NMR spectra are corresponded to hexane. Broadening effects of the peaks are observed due to oligomerization in ^{1}H NMR spectrum

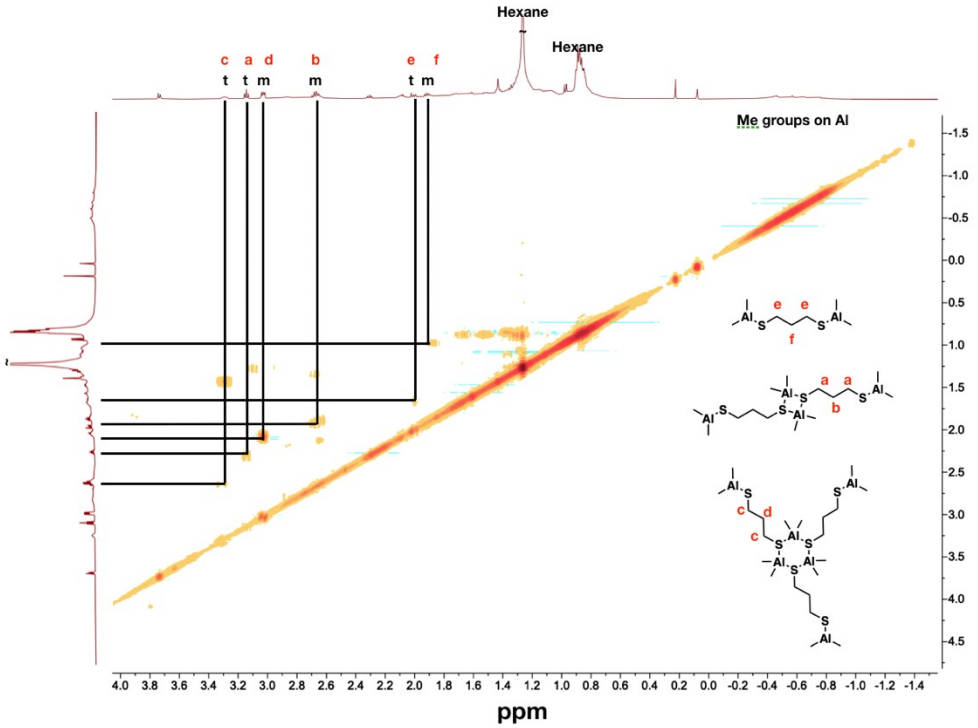

Figure S 20 ^{1}H–^{1}H correlation spectrum for d-H initiator. Only one half of the spectrum is shown for clarity. The spectrum suggests that there are three distinct species: single d-H initiator, dimerized, and trimerized form of d-H initiator, connect the peaks on the X- and Y-axes that are correlated with one another. The scheme below the diagonal represents the chemical structure of the species present. The peak assignments for the spectra are labeled here. Detailed peak assignments are listed in the methods section.

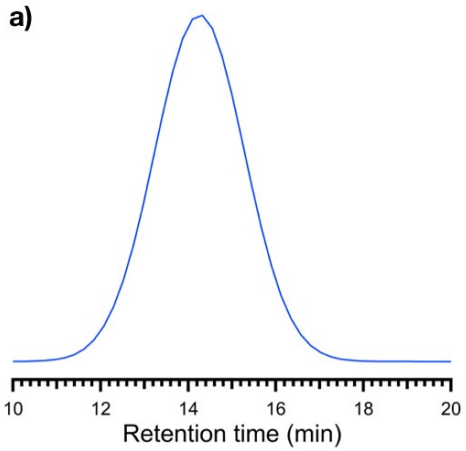

Figure S 21 SEC trace of d-h PPS. The M_n is determined to be 34.5 kg/mol with Đ of 1.37.

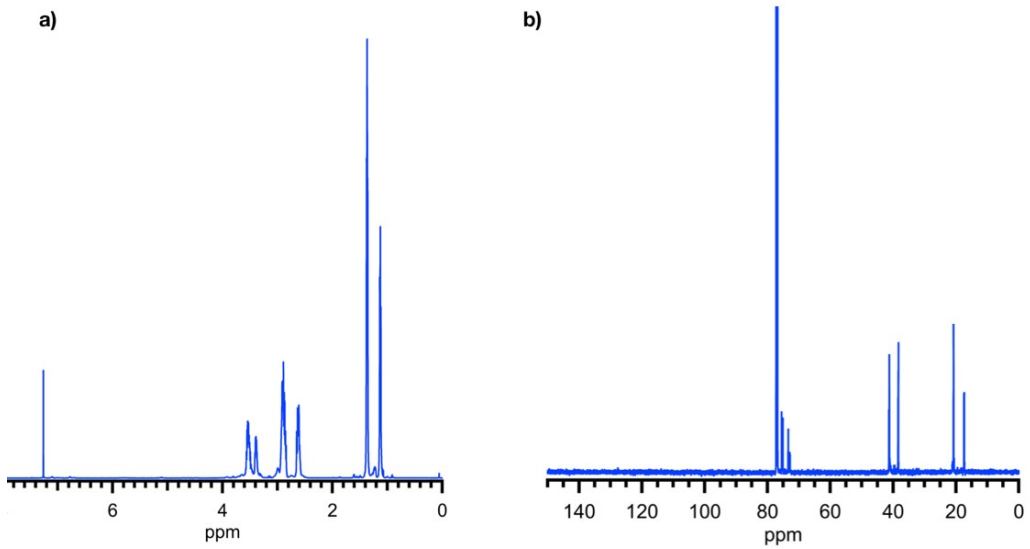

Figure S 22 ^{1}H NMR and ^{13}C NMR spectrum of d-H poly(PS-*b*-PO). (a) ^{1}H NMR (500 MHz, $CDCl_3$) δ 3.72−3.2 (bm, −O−C<u>H</u>$_2$−C<u>H</u>(CH_3)−O−), 2.91-2.54 (bm, −S−C<u>H</u>$_2$−C<u>H</u>(CH_3)−S−), 1.31 (m, −S−CH_2−CH(C<u>H</u>$_3$)−S−), 1.11 (m, −O−CH_2−CH(C<u>H</u>$_3$)−O−). (b) ^{13}C NMR (126 MHz, $CDCl_3$) δ 75.26 (−O−CH_2−<u>C</u>H(CH_3)−O−), 73.35 (−O−<u>C</u>H$_2$−CH(CH_3)−O−), 40.6 (−S−CH_2−<u>C</u>H(CH_3)−S−), 37.9 (−S−<u>C</u>H$_2$−CH(CH_3)−S−), 20.98 (−S−CH_2−CH(<u>C</u>H$_3$)−S−), 16.83 (−O−CH_2−CH(<u>C</u>H$_3$)−O−).

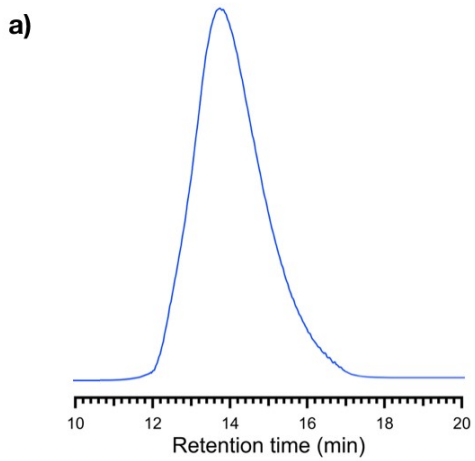

Figure S 23 SEC trace of d-H poly(PS-*b*-PO). The M_n is determined to be 29.8 kg/mol with Đ of 1.39.

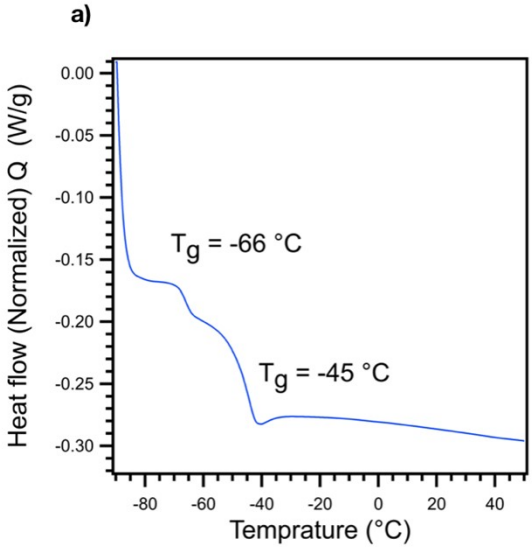

Figure S 24 DSC analysis of d-H poly(PS-*b*-PO). The data from the second heating curve were collected which reveals two Tgs at -66 °C and -45 corresponded to PECH and PPS blocks.

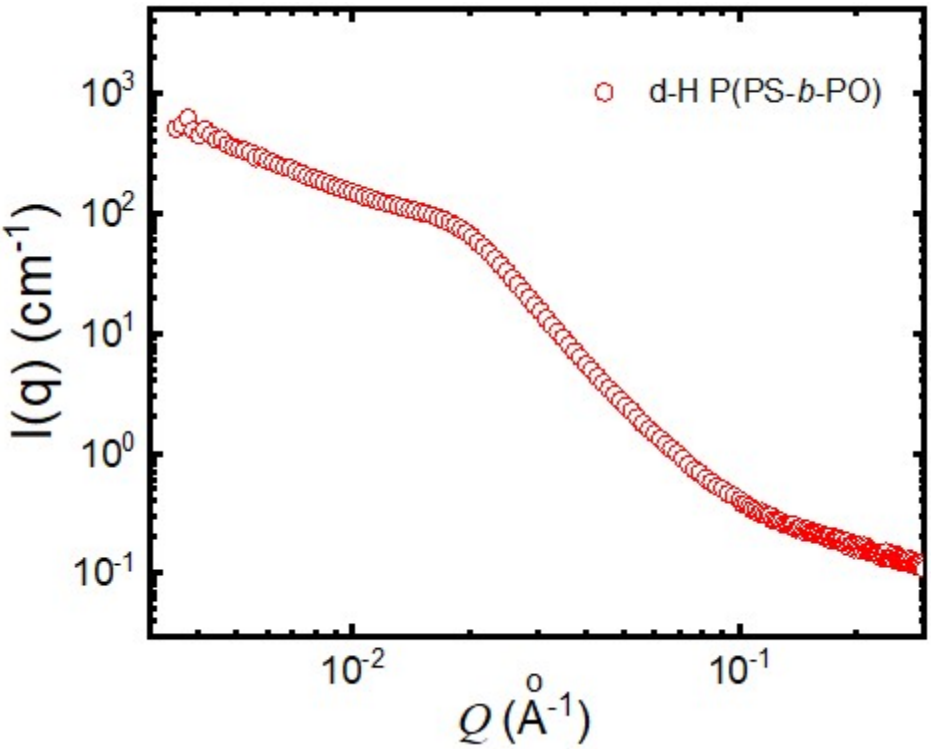

Figure S 25. SAXS data for the synthesized copolymer. The phase behavior of the d-H poly(PS-*b*-PO) reveals clear micro-phase separation for the block polymer synthesized with the d-H initiators with a notable peak at Q ~ 0.02 $Å^{-1}$ for d-H P(PS-b-PO).

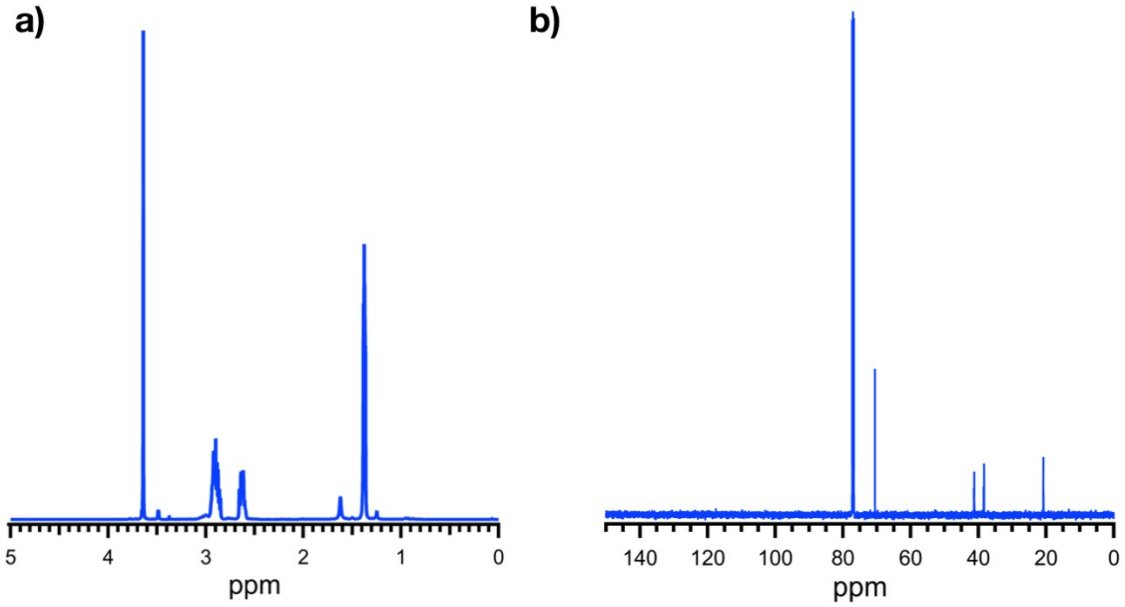

Figure S 26 ^{1}H NMR and ^{13}C NMR spectrum of PEG-*b*-PPS a) ^{1}H NMR (500 MHz, $CDCl_3$) δ 3.65-3.48 (b, −O−CH_2−CH_2−O−), 2.92-2.78 80 (m, −S−CH_2−CH(CH_3)−S−), 2.66-2.59 (m, −S−CH_2−CH(CH_3)−S−), 1.38 (m, −S−CH_2−CH(CH_3)−S−). b) ^{13}C NMR (126 MHz, $cdcl_3$) δ 70.55 (−O−CH_2−CH_2−O−), 41.26 (−S−CH_2−CH(CH_3)−S−), 38.38 (−S−CH_2−CH(CH_3)−S−), 20.79 (−S−CH_2−CH(CH_3)−S−).

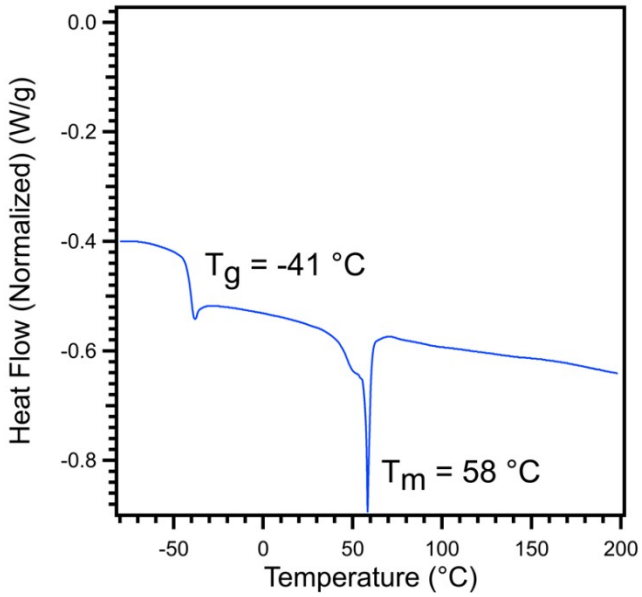

Figure S 27 DSC analysis of PEG-*b*-PPS. The data from the second heating curve were collected which reveals one T_g at -41 °C for PPS block and another T_m at 58 °C.

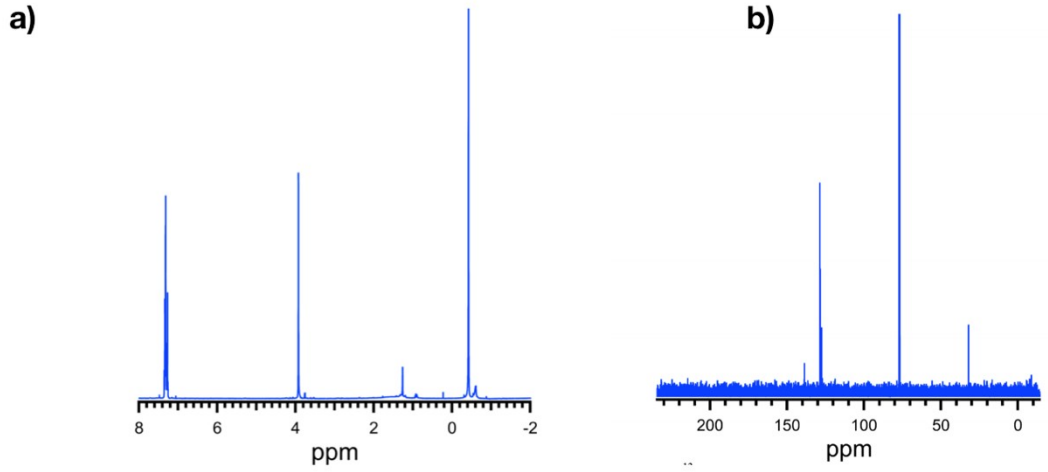

Figure S 28 ^{1}H NMR and ^{13}C NMR spectrum of $BnSAlMe_2$. a) ^{1}H NMR (500 MHz, $CDCl_3$) δ 7.38 – 7.21 (m, 5H, $\underline{Ph}CH_2S\text{-}Al(CH_3)_2$), 3.91 (s, 2H, $PhC\underline{H_2}S\text{-}Al(CH_3)_2$), -0.43 (s, 6H, $PhCH_2SAl(C\underline{H_3})_2$). b) ^{13}C NMR (126 MHz, $CDCl_3$) δ141.46, 128.56, 127.97, 126.89 ($\underline{Ph}CH_2S\text{-}Al(CH_3)_2$, 32.00 ($Ph\underline{C}H_2S\text{-}Al(CH_3)_2$), 28.78 ($PhCH_2S\text{-}Al(\underline{C}H_3)_2$).

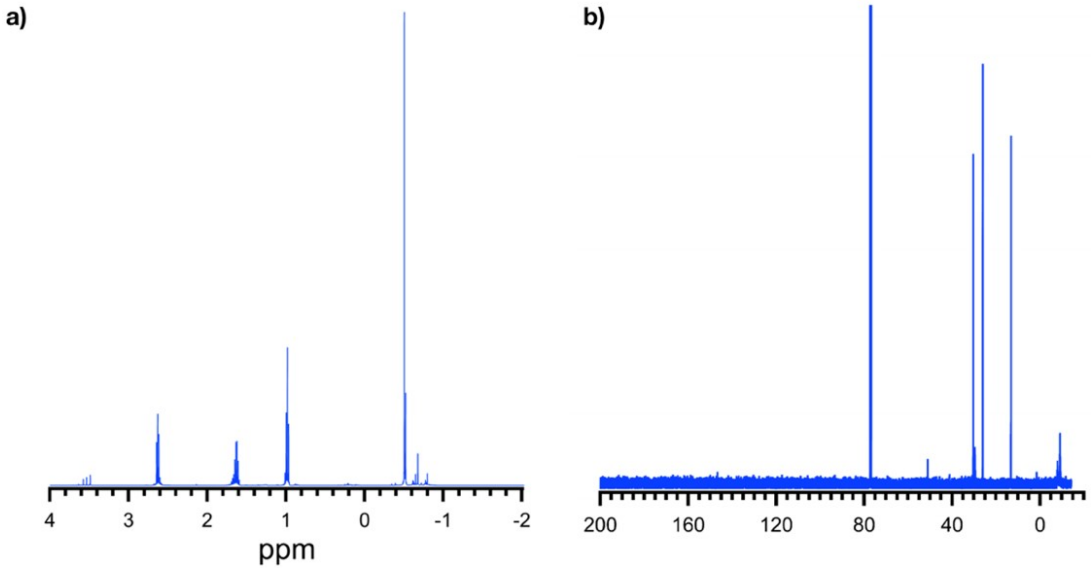

Figure S 29 ^{1}H NMR and ^{13}C NMR spectrum of $PrSAlMe_2$. a) ^{1}H NMR (500 MHz, $CDCl_3$) δ 2.62 (m, 2H, $CH_3CH_2C\underline{H_2}S\text{-}Al(CH_3)_2$), 1.65 (dq, 2H, $CH_3C\underline{H_2}CH_2S\text{-}Al(CH_3)_2$), 1.04-0.95 (m, 3H, $C\underline{H_3}CH_2CH_2S\text{-}Al(CH_3)_2$), -0.49 (S, 6H, $CH_3CH_2CH_2S\text{-}Al(C\underline{H_3})_2$). b) ^{13}C NMR (126 MHz, $CDCl_3$) δ 30.33 ($CH_3CH_2\underline{C}H_2S\text{-}Al(CH_3)_2$), 25.97 ($CH_3\underline{C}H_2CH_2S\text{-}Al(CH_3)_2$), 13.15 ($\underline{C}H_3CH_2CH_2S\text{-}Al(CH_3)_2$), -9.21 ($CH_3CH_2CH_2S\text{-}Al(\underline{C}H_3)_2$).

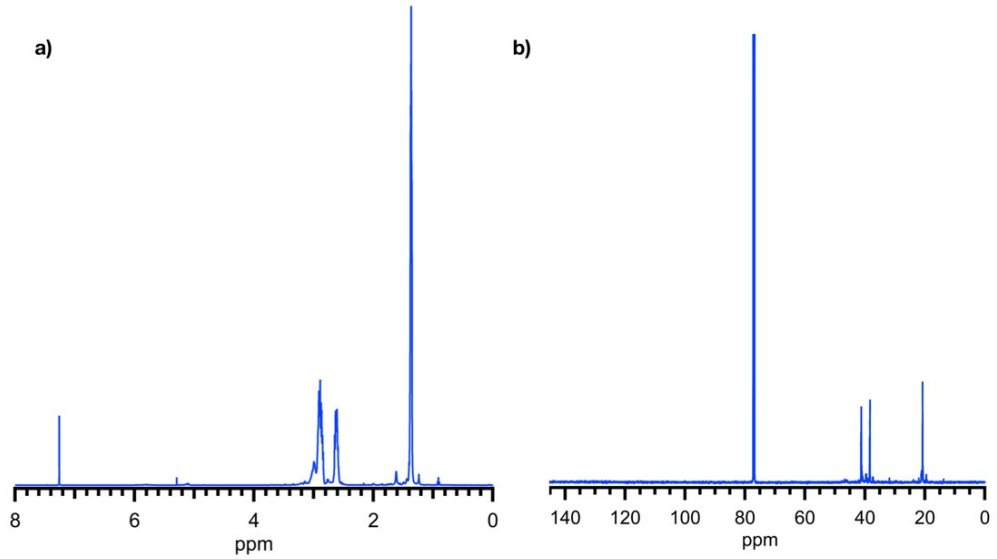

Figure S 30 ^{1}H NMR and ^{13}C NMR spectrum of d-H PPS. (a) ^{1}H NMR (500 MHz, $CDCl_3$) δ 2.91-2.80 (m, −S−C<u>H</u>$_2$−CH(CH_3)−S−), 2.65-2.58 (m, −S−CH_2−C<u>H</u>(CH_3)−S−), 1.39 (m, −S−CH_2−CH(C<u>H</u>$_3$)−S−). (b) ^{13}C NMR (126 MHz, $CDCl_3$) δ^{13}C NMR (126 MHz, $CDCl_3$) δ 41.14 (−S−CH_2−<u>C</u>H(CH_3)−S), 38.18 (−S−<u>C</u>H_2−CH(CH_3)−S), 20.63 (−S−CH_2−CH(<u>C</u>H_3)−S−).

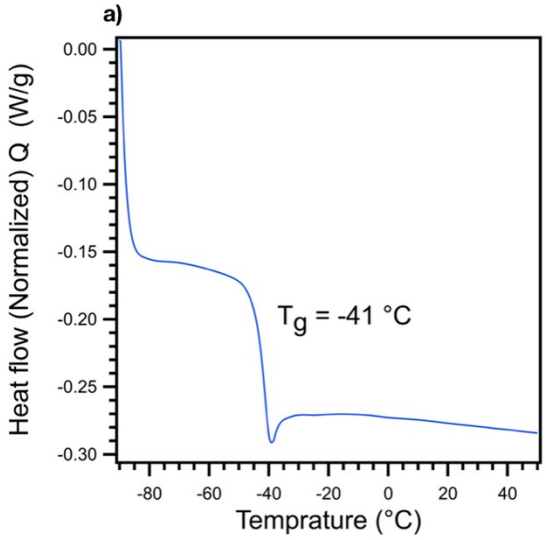

Figure S 31 DSC analysis of d-H PPS. The data from the second heating curve were collected which reveals one T_g at -41 °C.

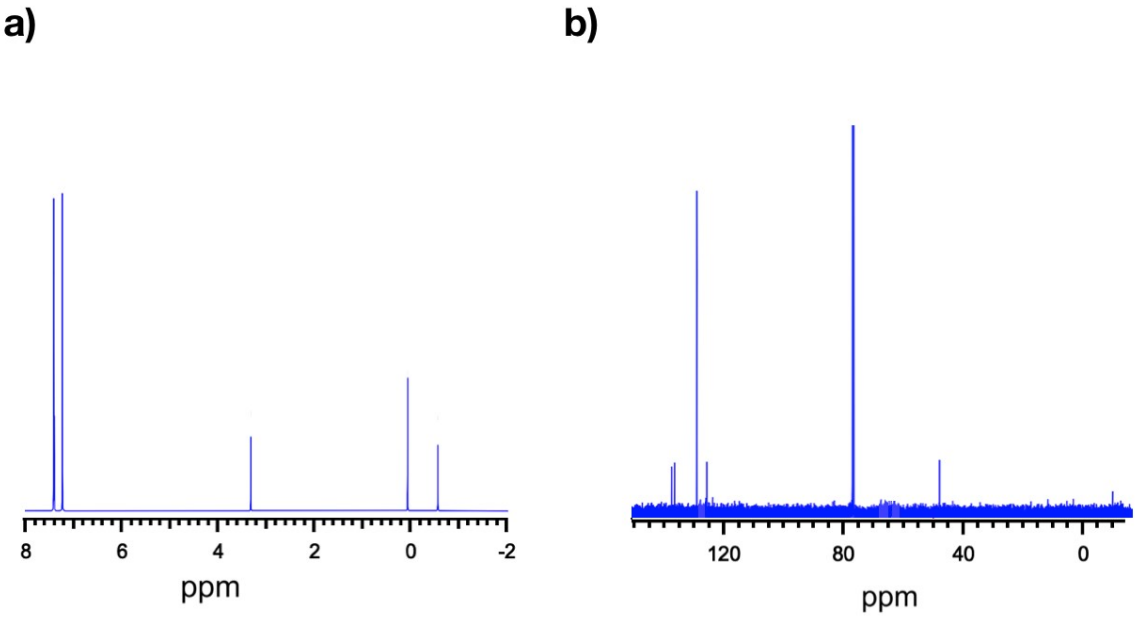

Figure S 32 ^{1}H NMR and ^{13}C NMR spectrum of $BnOAlMe_2$. a) ^{1}H NMR (500 MHz, $CDCl_3$) δ 7.47 – 7.38 (m, 5H, $\underline{Ph}CH_2O\text{-}Al(CH_3)_2$), 3.33 (s, 2H, $PhC\underline{H_2}O\text{-}Al(CH_3)_2$), 0.15 - -0.6 (s, 6H, $PhCH_2OAl(C\underline{H_3})_2$). b) ^{13}C NMR (126 MHz, $CDCl_3$) δ138.64, 137.57, 130.04, 126.69 ($\underline{Ph}CH_2O\text{-}Al(CH_3)_2$, 50.76 ($Ph\underline{C}H_2O\text{-}Al(CH_3)_2$), -7.71 ($PhCH_2O\text{-}Al(\underline{C}H_3)_2$).